Progress on the Development of High Spatial Resolution Imaging Techniques in Nuclear Medicine

Zhengrong Liang [1], Shanglian Bao, Jiangsheng You, Weidong Wang, and Guoping Han

Departments of Radiology, Physics and Astronomy, and Computer Science, State University of New York at Stony Brook, NY 11794, USA

The Institute of Heavy Iron Physics, Peking University, Beijing 100871, China

The PLA General Hospital, Beijing 100853, China

Abstract: Functional imaging of the human tissues has traditionally been performed using intravenous injection of radiotracers in the field of Nuclear Medicine. Quantitative assessment of the tracer concentration distribution across the body is the key for functional study of the tissues. Achieving high spatial resolution is the major task in developing the imaging modalities. This article reviews the current progress in the technology development, as well as our research work in the track.

Introduction

The dynamics of radioactivity inside the human body, introduced by intravenous injection as molecular tracers, reflects the functions of the tissues, such as physiology, metabolism, and *etc* [5]. The goal of single photon emission computed tomography (SPECT) and positron emission tomography (PET) is to image the radiotracer distribution for medical diagnosis and treatment [27]. PET has several advantages over SPECT, such as higher detection efficiency, better spatial resolution, and more suitable biological radiotracers. However, the cost limits its wide use in clinical settings. SPECT is cost effective and clinically advantageous.

A typical SPECT or PET study consists of three phases. The first phase is administration of a radiopharmaceutical, in which a suitable amount dose of isotope labeled radiopharmaceutical is injected into the patient.

The second phase is data acquisition, during which a detector system is placed and/or moved around the patient to collect γ emissions from inside the body. For SPECT imaging, an output image of a gamma camera is the projection of the three-dimensional (3D) radioactivity distribution on the detector surface, digitized in a two-dimensional (2D) pixel array. Many projections around the body are required to determine the radioactivity distribution. Let m be the number of views evenly spaced around the body. These m projections can be acquired either simultaneously in a time period Δt, or sequentially in a time period $m\Delta t$, or in a combination in a time period less than $m\Delta t$ (where $m\Delta t$ is much shorter than the half-life of the radiotracer). For PET, the measurement is on each paired detector elements in coincidence. Each measurement is the projection of the radioactivity source along the line connecting the paired detector elements (i.e., the line-of-response, LOR). By a ring detector around the body, all the measurements (or sinogram) on all the LORs in a time period Δt can be arranged into m projections from the source.

The final phase is image reconstruction, in which the concentration distribution of the injected radiotracer is estimated from the observed projection data (photon counts). In order to obtain a high quality image of the concentration distribution, several image degradation factors should be considered and compensated in image reconstruction. Among the degradation factors are noise in the projection data, Compton scatter, attenuation, system response (or collimator-detector response for SPECT) and, in cardiac imaging, the motion of heart. Additional factors for PET are random coincidence, movement of positron from the decay site, *etc*.

As a trivial example for the reconstruction problem, let's consider the difference between the simultaneous acquisition of m projections in a time period of Δt and the sequential acquisition of the m projections in a time period of $m\Delta t$. Due to the isotope decay, the sequential acquisition has a set of inconsistent linear equations

[1] Chinese Journal of Medical Physics, Vol.17, No.2, pp. 75-81, April, 2000. ISSN 1005-202X, CN 44-1351/R

determining the solution, while the linear equations for the simultaneous acquisition are consistent. More important issues will be addressed in the following sections.

Extraction of features from the reconstructed images is a clinically related task. We will not discuss this aspect in this article.

Progress on SPECT Research

Brain SPECT

The most popular camera-based SPECT systems use a single or multiple scintillation cameras that are mounted on a rotating gantry. Recently multiple camera-based SPECT systems became increasingly more popular because of their increased sensitivity per image slice. A triple-camera system is sketched in Figure 1 below. To further increase the sensitivity, fan-beam collimators instead of conventional parallel-hole collimators can be used. A fan-beam collimator is depicted in Figure 2.

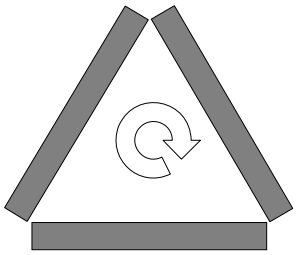

Figure 1. Triple camera system

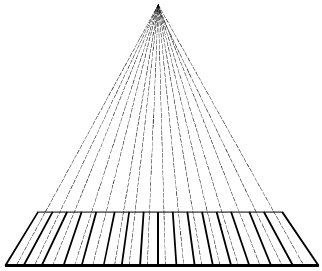

Figure 2. Fan beam collimator

Various image degradation factors present in a real imaging situation, including noise, scatter, system response, and attenuation should be considered and compensated in the reconstruction of the concentration distribution. A comprehensive study on parallel-hole collimated SPECT brain imaging was detailed in [16].

To accurately model the noise in projection data, the noise characteristics should be studied first. Although the assumption of Poisson noise and independence of measurements among detector bins is widely accepted, only until recently, the assumption was mathematically formulated based on a 4D Poisson impulse field model for parallel-beam projection data [38]. A noise model for fan-beam projection data is currently under investigation.

The classic noise suppression in SPECT is to apply a low-pass filter with different windows and cutoff frequencies, where the location of the cutoff frequency and the type of window determine the trade-off between image noise and spatial resolution. A drawback in this approach is that it is impossible to determine the optimal window and cutoff frequency without prior information. Recently we have investigated a noise suppression approach with the Wiener filter that considers the Poisson noise characteristics accurately [4]. In this work, the noise in the projection data is assumed to be Poisson and therefore signal dependent. However, the Anscombe transform of the projection data is well approximated by a Gaussian distribution with a signal independent variance (a constant of 0.25) [1]. For the Gaussian variable with constant variance, a Wiener filter can be accurately constructed. After noise smoothing with the Wiener filter, the inverse Anscomb transform is applied. Further research on spectrum estimation for the Wiener filter is needed. Some alternative approaches for noise reduction can be found in [19,22].

Compensation of the Compton scatter has been addressed by several articles. One of the popular methods is the use of a triple energy-window acquisition protocol [21]. The photons detected at each detector bin are grouped according to their energies into three distinct windows, one main window in the center and two sub-windows below and over the main window. For example, in SPECT studies with Tc-99m labeled radiopharmaceuticals, the main window can be set in the range from 128 to 152 keV and the two sub-windows from 124 to 128 keV and from 152 to 156 keV, respectively. The counts in both the main and sub-windows should be smoothed [4], respectively, and then linearly combined to estimate the scattered counts in the main window. The estimated

scattered counts are then subtracted from the main window counts. A comprehensive investigation on the estimation accuracy by point source experiments in water is detailed in [12].

Correction of the spatially variant collimator/detector response for resolution improvement can be achieved by either the distance-frequency relation [10] or the inversion approach [29]. The former approximates the deconvolution formula, but considers the resolution variation kernel accurately. The later one approximates the kernel's functional for the mathematical formula. Our experiments show that the former approach is a better choice for the resolution improvement [11].

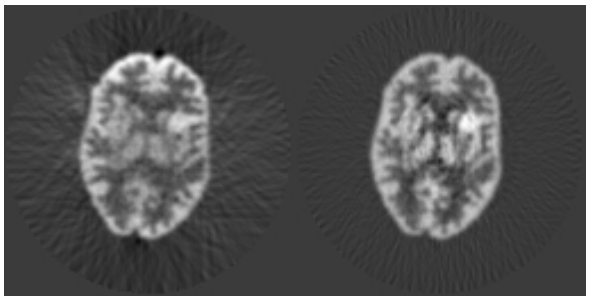

Figure 3. Comparison of our quantitative SPECT reconstruction (right) with the conventional FBP reconstruction (left) for the 3D Hoffman brain model. Our analytical approach achieved the quantitative reconstruction of 128×128×32 array size in less than 5 minutes by a HP/735 desktop computer without transmission scans (although transmission scans are usually required for photon attenuation compensation in SPECT).

For brain studies, the head attenuation can be well approximated as constant, with the skull replaced by an equivalent brain tissue via enlargement of the head contour. Instead of determining the variable head attenuation map from a transmission scan, we determine the head contour by the use of the scattered photon counts from the sub-windows. Experiments have demonstrated that accurately determination of the head contour is feasible [7]. In this method, the filtered backprojection (FBP) reconstruction algorithm is performed on the estimated scatter data from the sub-windows. The reconstructed image is smoothed and then thresholded to determine the boundary of the head. An alternative is to determine the head boundary directly from the projection data of the sub-windows [6]. Since the attenuation factors of the skull along the radial directions are dependent on the radius of the skull from the center, a radially enlargement of the contour will compensate for the skull attenuation [16]. With a slightly tilted head for the data acquisition (in order to avoid cavity in the field-of-view (FOV)) and an enlarged uniform attenuation map, the head attenuation can be accurately compensated in the inversion of the exponential Random transform for the source distribution. The mathematical derivation assumes that the radiotracer is inside the brain tissues (not in the skull), this is usually the case in clinic. It is clear that the extra transmission scan for head attenuation map is not necessary. Some experimental results from the Hoffman brain phantom imaging are given by Figure 3 above.

Iterative reconstruction for brain SPECT imaging may not offer any advantage, as compared to the above analytical approach. However, research in other aspects can improve the spatial resolution. One is the improvement of the location of γ interaction inside the NaI(Tl) crystal in the gamma camera [30]. A carefully designed collimator geometry for improved detection efficiency and spatial resolution will be a very interesting research topic to advance the imaging quality. For example, the fan-beam geometry of Figure 2 will increase the sensitivity due to its fully use of the detector crystal and the spatial resolution due to its amplification of imaged object on the collimator surface. A comprehensive study on the noise, scatter, collimator response, and attenuation for the fan-beam geometry of Figure 2 is our current research interest [37].

Chest SPECT

For chest SPECT imaging, three distinct factors from the brain studies should be considered. One is the large size of the chest, as compared to the head. The second is the motion of the heart. The last one is the significant different attenuation of the lungs from the surrounding tissues. While fan-beam collimators increase sensitivity and resolution in brain SPECT imaging, they cause truncation problems when applied to cardiac and pulmonary

studies. Therefore, the parallel-hole collimators are widely used for clinic in current time. Obviously, the triple-camera SPECT system of Figure 1 is not optimal for chest imaging. The dual-camera vertex system of Figure 4 below is presently a choice for chest SPECT imaging.

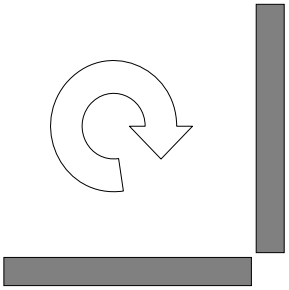

Figure 4. Dual head vertex system.

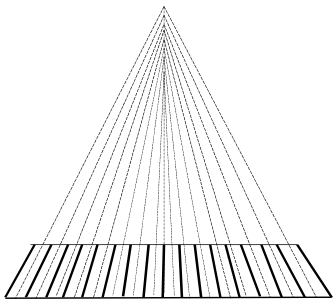

Figure 5. Variable focal length fan-beam collimator.

To take the advantage of fan-beam collimator, while avoiding the truncation problems, a variable focal-length fan-beam collimator of Figure 5 can be a choice [35,36]. This collimator increases the sensitivity and resolution (as the fan-beam collimator does) and does not have the truncation problems (as the parallel-hole collimator does). A comprehensive study on the noise, scatter, collimator response, and attenuation for this complicated collimator geometry for chest SPECT imaging is our another current research interest [37,38].

The gated SPECT imaging through the cardiac circle can minimize the effects due to the heart motion. The cardiac cycles can be monitored by the ECG signals. Each cardiac cycle is divided into several (e.g. 12 or 16) time slots. Photon counts detected in different time slots are accumulated in different frames. Each frame consists of a number (e.g., m) of projection data. An image reconstruction can be applied to the m projections to get the time-averaged concentration distribution in each corresponding phase in the cardiac cycle. One major drawback of this simple reconstruction approach is the low counts in each phase and hence poor spatial resolution and image quality. Recently, a new method using the KL transform has been proposed to deal with this problem [31]. The idea is that the counts in different frames are related and can be combined in some way to increase the sensitivity.

Similar to the brain SPECT imaging, the degradation factors due to photon detection must be taken into account and compensated in the image reconstruction. Here the attenuating non-uniformity due to the lungs makes analytical inversion impossible. Therefore, iterative image reconstruction plays a major role here. Statistical modeling of the noise and treatment of the deterministic factors were detailed in [18] for parallel-hole collimated chest SPECT imaging.

Noise characteristics for parallel-hole collimator are well established and can be mathematically described by a 4D Poisson impulse field model [38]. The measured projection data are mutually independent Poisson variables. While the characteristics of the noise in varying focal-length fan-beam projection data are not clear, it is conjectured that the projections are also mutually independent Poisson variables. Therefore, the probability density function of the measurements is written as a Poisson likelihood function. It would be expected that the maximum likelihood (ML) estimate of the probability function should generate a significantly improved result, as compared to the FBP method, because the Poisson noise is accurately modeled in the likelihood function [24]. Practically, this is not the case. Including *a priori* source information for a maximum *a posteriori* (MAP) solution, via the Bayesian inference, should improve the reconstruction quality [13]. Here the use of valid *a priori* information is the key issue.

Treatment of the non-uniform attenuation, scatter, and spatially variant detector/collimator response is included in the projection and backprojection circle of iterative reconstructions. The object-specific attenuation map is necessary and can be obtained by a transmission scan. Two external scanning line sources across the FOV for two detectors of the SPECT system (see Figure 4) can provide the completely sampled transmission data. A FBP reconstruction will generate the attenuation map. Then attenuation and scatter compensations are performed based on the reconstructed map [17]. Inclusion of detector/collimator response kernel in the iterative circle can be very efficiently accomplished using the local convolution modeling [17].

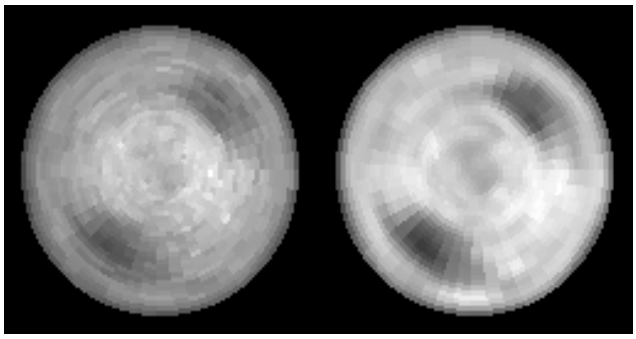

Figure 6. A 2D mapping (or Bullseye Display) of the 3D myocardium function from myocardial perfusion SPECT. For a normal heart, the display would be relatively uniform. On the left is the conventional FBP reconstruction of the myocardium function, where two defects are barely seen. On the right is the result of our quantitative reconstruction (of 128 cubic size) which was accomplished in less than 15 minutes on a HP/735 desktop computer.

Some hybrid approaches have been considered to improve the computational efficiency. One example is given here, following the treatment procedure described in the brain SPECT above. We can smooth the noise first by the Wiener filter [4], then perform the scatter estimation and subtraction [12], and further execute the deconvolution [10]. Finally we compensate for the non-uniform attenuation in the iterative reconstruction of the source distribution [34].

Some experimental results from a chest phantom imaging using parallel-hole collimators are given by Figures 6 above. Further investigation on the noise characteristics in variable focal-length fan-beam collimator is under progress [38]. A new model is being studied for the complicated collimator response [37]. Efficient image reconstruction with compensation for the non-uniform attenuation in this complicated geometry is also in the progress [6].

Other researches in SPECT instrumentation and image formation algorithm include: (1) The use of more efficient detector materials, such as semiconductors [9]. (2) Design of alternative collimator geometry, such as cone-beam collimator [8]. (3) New image formation mechanism, such as Compton scatter camera [25,26]. And (4) more accurately modeling of the photon detection physics and more efficiently accomplishing the models in currently available computing environment. For example, a microSPECT can achieve less than 1 mm resolution for imaging of a small object less than 5 cm in size by the pin-hole collimators [27].

Progress on PET Research

Since PET image reconstruction is much easier than that of SPECT, most research effort has been devoted to instrumentation. In recent years, a number of crystal inorganic scintillators have been discovered and studied for use in high resolution PET, including cerium-doped gadolinium oxyorthosilicate (GSO(Ce)) [28], yttrium oxyorthosilicate (YSO) [2], bismuth germanate (BGO), cerium-doped lutetium Oxyorthosilicate (LSO(Ce)) [2,3], *etc*. These crystal inorganic scintillators generally have significantly improved the detection performance for the 511 keV high energy γ rays, as compared with the NaI(Tl) material, in one or more aspects for PET. For example, LSO has much shorter decay time than NaI(Tl) and can be employed to reduce the dead time. BGO, GSO and LSO all have shorter radiation length and can be used to improve the spatial resolution and to reduce the size and the fabrication cost of the crystals. They also have very high gamma-ray detection efficiency due to their high density and high effective atomic number. The ruggedness of BGO and LSO also facilitates handling and packaging. Also, all these crystal inorganic scintillators are non-hygroscopic, in contrast to NaI(Tl). Perhaps the only drawback of these crystals is that they have somewhat lower emission intensity than NaI(Tl).

Yamamoto studied a method to improve PET resolution by using tapered fiber, a fiber optical plate whose output surface is larger than the input surface, optically coupled to the crystal in the front and to a position sensitive photomultiplier tube (PMT) in the back [32]. Because of the amplification of the light photon image by the tapered fiber, remarkable spatial resolution was achieved in his experiments with a N-22 coin source and 8×8 matrix of 2.5 mm BGOs and 11×11 matrix of 1.65 mm BGOs.

To restore spatial resolution uniformity in PET and to increase sensitivity at lower fabrication costs through a reduction of the tomograph ring radius, the development of position encoding detectors with depth-of-interaction (DOI) sensitivity is under hot discussion.

Miyaoka et al proposed and evaluated a method to determine DOI from a PET detector module that controls the light sharing between neighboring crystals and extract the DOI information from the ratio of the light collected using simple Anger type logic [20]. To control the light sharing, the interface between crystals was specially designed so that a significant amount of light is shared when a photon interacts near the front face of a crystal and very little light is shared when an interaction occurs near the back of a crystal. For that purpose, they use optical coupler between crystals near the front face, opaque reflector near the back, and moderately opaque material in between the front face and the back. Also, the front section of the detector, where most of the interactions occur, is designed to be more sensitive to DOI effects, using a separate crystal optically coupled to a crystal in the back end.

Another method to determine the DOI, as proposed recently by Yamamoto et al [33], tries to employ the property of GSO(Ce) that its decay time can be controlled by the concentration of Ce. In their proposed design of the block detector, GSO crystals in the front, the middle and the back are differently doped with Ce. The pulse shape discrimination or zero-cross time peak channels would tell the interacting crystal and thus determine the DOI.

The collection efficiencies of light photons from interactions at different depths are slightly different, and the distributions of the pulse height are also different. Rogers observed this fact and presented a method that uses an empirically determined, tabulated relationship between DOI and the most probable pulse-height to estimate the unknown depth from the measured pulse-height for each detected gamma ray [23].

A typical block-modulated PET detector crystal is shown by Figure 7 below. Several blocks along the z-axis (normal to the ring) for a multi-ring detector system (see Figure 8) could acquire more than 60 slice images. This greatly advanced the volume imaging in real time.

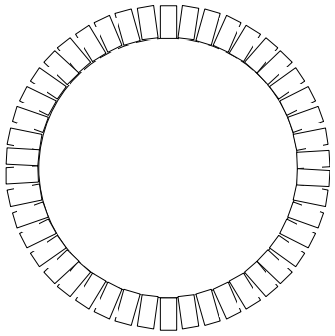

Figure 7. A module of crystal elements and PMTs.

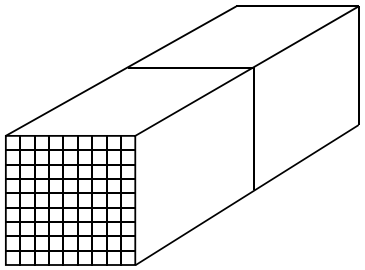

Figure 8. A ring system of detector modules.

For attenuation correction, a radioactive rod source closed to the inner surface of the ring is usually used to acquire the transmission data. The attenuation correction can be performed in the projection space along all the LORs. Correction for the random coincidence and deadtime is done during the data acquisition. Scatter compensation is a challenged problem, although scatter estimation using off-peak energy windows has made some progress.

We have studied the effect of the non-uniform detector response due to the mislocation of interaction events inside the detector crystal and the non-uniform sampling of the detector elements across the FOV [15]. A spatially variant restoration for the uniform sampled data from the measured sinogram is performed first, based on a MAP approach. After the restoration, reconstruction of image is straightforward by the FBP method. The results are extremely encouraging, as shown by Figures 9, 10, and 11.

A new image-formation concept was studied by this research group [14]. The isotope Fe-52 emits a positron and a gamma photon simultaneously. By the principle of the Compton scatter camera [25], the detection of the gamma photon will determine a cone surface in the source space, in which the decay may occur, see Figure 12.

The PET detection of the pair photons from the positron annihilation will determine a LOR in the source space. Figure 13 depicts the detector configuration. The intersections of the cone surface and the LOR are at two points, and most times there is only one intersecting point (the other one is out of the FOV). By this concept, the image reconstruction may be unnecessary.

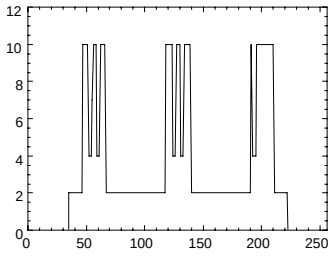

Figure 9. Phantom and profile.

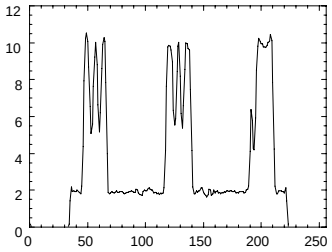

Figure 10. Reconstruction without restoration and profile.

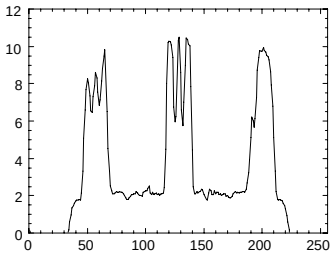

Figure 11. Reconstruction with restoration.

Sophisticated animal system is another research area for high resolution PET, where the spatial resolution can be less than 2 mm in FOV of less than 10 cm.

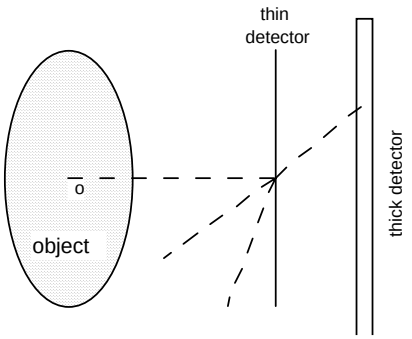

Figure 12. A photon emitted from point O in the object will be scatter (only once) by the thin detector and then detected by the thick detector. The two interaction sites determine a line. The energy deposited in the thin detector will give the scatter angle. So a cone surface is given with the line being its axis.

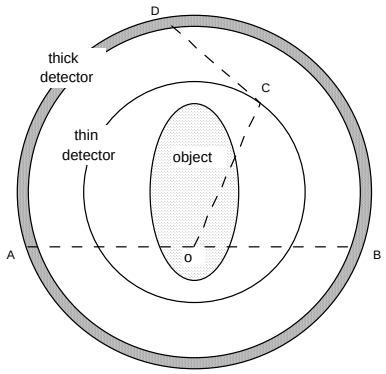

Figure 13. A double ring detector system for detection of triple photon emissions. The cone surface from the single photon detection and the line from the pair photon detection intersect at two points for the emission site.

Future Research Area

SPECT

As mentioned above, SPECT instrumentation is one aspect for further researches to improve the spatial resolution, which covers new detector material and collimator geometry. The development of clinically specific radiopharmaceuticals is another very important research aspect. This later aspect will play a very important role for patient diagnosis, treatment, and management. Off course, the image reconstruction for improved detector system

is also an important research aspect. Quantitative reconstruction of the radiotracer concentration in each voxel will improve the patient diagnosis and the assessment of the treatment effectiveness.

Dynamic imaging of the heart is a very challenging task and will attract a great research attention in the future.

PET

PET instrumentation is the critically important issue in the future research for improved spatial resolution. Real time reconstruction of whole body PET image is a very challenging problem and is also a clinically important task, especially for assessment of treatment effectiveness.

PET/SPECT dual imaging modality is another research topic which is currently under progress. One of these researches is the use of two gamma cameras (without collimators) for coincidence detection. The advantage is its large coverage along the rotation axis, in addition to its low cost. Therefore, it may be more efficient for whole body imaging. Another one is the use of phoswish detector configuration of Figure 7. The detector consists of a YSO layer in front of a LSO layer, and can detect both low-energy (140 keV) and high-energy (511 keV) photons. In detection of 140 keV photons, the events in LSO will be discarded, where LSO acts as a pass way for scintillation light to reaching photomultiplier tubes (PMTs). In this mode, the efficiency is compromised. In detection of 511 keV photons, both YSO and LSO will generate the events. This dual imaging modality may be unable to improve the image quality. Its practical value depends on the clinical use.

Acknowledgement

This work was supported by NIH Grant #HL54166 of the National Heart, Lung, and Blood Institute; Grant #NS33833 of the National Institute of Neurological Disorders and Stroke; Grant #CA79180 of National Cancer Institute; and Established Investigatorship of the American Heart Association.

References

[1] Anscomb, "The transform of Poisson, binomial and negative-binomial data," *Biometrika*, vol. 35, 246-254, 1948.

[2] C.D. Brandle, A.J. Valentino, and G.W. Berkstresser, "Czochralski growth of rare-earth oxyorthosilicates (Lu2SiO5)," *J. Crystal Growth*, vol. 79, 308-315, 1986.

[3] M.E. Casey, L. Eriksson, M. Schmand, et. al., "Investigation of LSO crystals for high resolution positron emission tomography," *IEEE Trans. Nucl. Sci.*, vol. 44, 1109-1113, 1997.

[4] J. Cheng, Z. Liang, J. Li, J. Ye, and D.P. Harrington, "Inclusion of *a priori* information in frequency space for quantitative SPECT imaging," *Conf Record IEEE NSS-MIC*, vol. 2, 1648-1652, 1997.

[5] P.J. Early, and D.B. Sodee, *Principles and Practice of Nuclear Medicine*, 2nd ed., St. Louis: Mosby, 1995.

[6] G. Han, J. You, and Z. Liang, "EM reconstruction with non-uniform attenuation in varying focal-length fan-beam collimated SPECT," *SUNY-SB, IRIS Lab Report*, 1998.

[7] X. Hao, G. Han, J. You, and Z. Liang, "Accurate determination of the head boundary from scatter data for analytical inversion of the exponential Radon transform," *SUNY-SB, IRIS Lab Report*, 1998.

[8] R.J. Jaszczak, C.E. Floyd, Jr., S.H. Manglos, K.L, Greer, and R.E. Coleman, "Cone beam collimation for single photon emission computed tomography: analysis, simulation, and image reconstruction using filtered backprojection," *Med. Phys.*, vol. 13, 484-489, 1986.

[9] L. Kaufman, K. Hosier, V. Lorenz, D. Shosa, J. Hoenninger, A. Cheng, M. Okerlund, R.S. Hattner, D.C. Price, S. Williams, J.H. Ewins, G.A. Armantrout, D.C. Camp, and K. Lee, "Imaging characteristics of a small germanium camera," *Investigative Radiology*, vol. 13, 223-232, 1978.

[10] R.M. Lewitt, P.R. Edholm, and W. Xia, "Fourier method for correction of depth dependent blurring," *SPIE Medical Imaging III*, vol. 1092, 232-239, 1989.

[11] J. Li, Z. Liang, J. Ye, and G. Han, "An investigation on analytical methods for correction of distance-dependent resolution variation in 3D SPECT imaging," *Conf Record IEEE NSS-MIC,* 1998 (to appear).

[12] L. Li, J. Li, G. Han, and Z. Liang, "Analysis of point-source measurements for PSF construction and scatter compensation," *SUNY-SB, IRIS Lab Report*, 1998.

[13] Z. Liang, R.J. Jaszczak, C.E. Floyd, and R.E. Coleman, "Bayesian reconstruction for SPECT: validation with Monte Carlo simulation, experimental phantom, and real patient data," *Inter. J. Imaging Sys. Tech.*, vol. 1, 149-168, 1989.

[14] Z. Liang, and R. Jaszczak, "Comparisons of multiple photon coincidence imaging techniques," *IEEE Trans. Nucl. Sci.*, vol. 37, 1282-1292, 1990.

[15] Z. Liang, "Detector response restoration in image reconstruction of high resolution positron emission tomography," *IEEE Trans. Med. Imaging*, vol. 13, 314-321, 1994.
[16] Z. Liang, J. Ye, J. Cheng, and D.P. Harrington, "Quantitative brain SPECT in three dimensions: an analytical approach without transmission scans," in P. Grangeat and J.L. Amans eds., *Three-Dimensional Image Reconstruction in Radiology and Nuclear Medicine*, 117-131, 1996.
[17] Z. Liang, J. Ye, J. Cheng and J. Li, "A new model for tracing first-order Compton scatter and central-ray attenuation in quantitative SPECT imaging," *Conf Record IEEE NSS-MIC* vol. 2, 1425-1429, 1996.
[18] Z. Liang, J. Ye, J. Cheng, J. Li, and D.P. Harrington, "Quantitative cardiac SPECT in three dimensions: validation by experimental phantom studies," *Phys. Med. Biol.*, vol. 43, 905-920, 1998.
[19] C.E. Metz, and X. Pan, "A unified analysis of exact methods of inverting the 2-D exponential Radon transform, with implications for noise control in SPECT," *IEEE Trans. Med. Imaging*, vol. 17, 643-658, 1995.
[20] R.S. Miyaoka, T.K. Lewellen, H. Yu, and D.L. McDaniel, "Design of a depth of interaction (DOI) PET detector module," *IEEE Trans. Nucl. Sci.* vol. 45, 1069-1073, 1998.
[21] K. Ogawa, Y. Harata, T. Ichihara, A. Kubo, and S. Hashimoto, "A practical method for position-dependent Compton-scatter correction in SPECT," *IEEE Trans. Med. Imaging*, vol. 10, 408-412, 1991.
[22] X. Pan and C.E. Metz, "Analysis of noise properties of a class of exact methods of inverting the 2D exponential Radon transform," *IEEE Trans. Med. Imaging*, vol. 17, 659-668, 1995.
[23] J.G. Rogers, "A method for correcting the depth of interaction blurring in PET cameras," *IEEE Trans. Med. Imaging*, vol. 14, 146-150, 1995.
[24] L.A. Shepp, and Y. Vardi, "Maximum likelihood reconstruction for emission tomography," *IEEE Trans. Med. Imaging*, vol. 1, 113-122, 1982.
[25] M. Singh, "An electronically collimated gamma camera for single photon emission computed tomography. Part I: theoretical considerations and design criteria," *Med. Phys*., vol. 10, 421-425, 1983.
[26] M. Singh, and D. Doria, "An electronically collimated gamma camera for single photon emission computed tomography. Part II: image reconstruction and preliminary experimental measurements," *Med. Phys*., vol. 10, 426-435, 1983.
[27] J.A. Sorenson, and M.E. Phelps, *Physics in Nuclear Medicine*, Philadelphia: W.B. Sanders, 1987.
[28] K. Takagi, and T. Fukazawa, "Cerium-activated Gd2SiO5 single crystal scintillator," *Appl. Phys. Lett.,* vol. 42, 43-45, 1983.
[29] L. van Elmbt, and S. Walrand, "Simultaneous correction of attenuation and distance-dependent resolution in SPECT: an analytical approach," *Phys. Med. Biol.*, vol. 38, 1207-1217, 1993.
[30] W. Wang, S. Bao, and J. Cai, "Investigation on the delay weighting method for the position estimation of gamma photon," *Acta Electronica Sinia*, vol. 26, 96-99, 1998.
[31] M.N. Wernick, E.J. Infusino, and C.M. Kao, "Fast optimal pre-reconstruction filters for dynamic PET," *Conf Record IEEE NNS-MIC*, CD-ROM, 1998.
[32] S. Yamamoto, "Resolution improvement using tapered fiber for a high resolution PET block detector," *IEEE Trans. Nucl. Sci.*, vol. 45, 1074-1077, 1998.
[33] S. Yamamoto, and H. Ishibashi, "A GSO depth of interaction detector for PET," *IEEE Trans. Nucl. Sci.*, vol. 45, 1078-1082, 1998.
[34] J. Ye, Z. Liang, and D.P. Harrington, "Quantitative reconstruction for myocardial perfusion SPECT: an efficient approach by depth-dependent deconvolution and matrix rotation," *Phys. Med. Biol.*, vol. 39, 1263-1279, 1994.
[35] J. You, S. Bao, and Z. Liang, "Benefits of angular expression to reconstruction algorithms for collimators with spatially varying focal lengths," *IEEE Trans. Med. Imaging*, vol. 16, 527-531, 1997.
[36] J. You, Y. Li, and S. Bao, "Image reconstruction from variable focal-length fan-beam projections", *J. Imaging and Graphics*, vol.3, 666-669, 1998.
[37] J. You, and Z. Liang, "Least square algorithm for compensation of collimator response using circular harmonic decomposition in projection space: I: theory," *SUNY-SB, IRIS Lab Report*, 1998.
[38] J. You, G. Han, and Z. Liang, "A Poisson impulse field analysis on noise propagation for SPECT imaging," *SUNY-SB, IRIS Lab Report*, 1998.